JOURNAL OF MATERIALS SCIENCE 35 (2000) 4695–4703

High-temperature oxidation of Fe_3Al containing yttrium

INSOO KIM, W. D. CHO
Department of Metallurgical Engineering, University of Utah, Salt Lake City, UT 84112, USA
E-mail: w.cho@m.cc.utah.edu

H. J. KIM
Department of Mechanical Engineering, Yuhan College, Puchon City, Kyungki-Do, 422-749, South Korea

The effect of yttrium addition on the oxidation behavior of Fe_3Al alloys was investigated in terms of oxidation rate and oxide adhesion in the temperature range of 800 to 1100 °C. The oxidation rate of the alloys, Fe-14.3 wt% Al and Fe-14.1 wt% Al-0.3 wt% Y, was nearly identical, and the parabolic rate constant as a function of temperature is found to be $K_p = 5128 \exp[-39506\ (\text{cal/mol})/RT]\ \text{mg}^2/\text{cm}^4$ hr. While the alumina scale formed on the Y-free Fe_3Al alloy was observed to be fragile and spalled easily, the oxide layer formed on the Fe_3Al-Y was protective, dense, and adhesive. Based on the microstructural, morphological, and compositional studies, the adhesion improvement due to the yttrium addition was discussed in terms of growth stress, the formation of pegs and scale growth mechanism. © *2000 Kluwer Academic Publishers*

1. Introduction

Iron aluminides have attracted the attention of many researchers as candidates for high-temperature structural materials mainly because of their excellent oxidation resistance due to the formation of protective alumina scale. In order to resist aggressive environments at elevated temperatures, oxide scale formed on iron-aluminum alloy must satisfy the following three requirements: (1) thermodynamic stability, (2) slow growth rate, and (3) adherence on the substrate. According to Wallwork and Hed [1], the most suitable alloys for high-temperature applications are Fe, Ni, and Co alloys with the respectively protection of SiO_2, Cr_2O_3, and $A1_2O_3$ scales. While chromium oxide can vaporize as CrO_3 at the temperatures above 1000 °C and silicon oxide may form low melting silicate [2, 3], $A1_2O_3$ is thermodynamically stable at high temperatures and has higher melting point. In this respect, the alloys forming alumina, such as iron aluminides, seem to be most suitable for use at high temperature. However, alumina scale formed on the iron-aluminum alloys tends to be easily spalled during oxidation due to the growth stress and thermal stress.

It has been known that the addition of small amounts of reactive element, such as Y or Ce, to chromia- and alumina forming alloys improves the adhesion of the oxide to the substrate. Ramanarayanan *et a1*. [4–6] investigated the influence of yttrium on oxide scale growth and adherence of alumina formed on various alloys. They reported that the presence of yttrium reduced growth stresses arising from Al_2O_3 nucleation within an existing scale and, thus, greatly improved the scale adhesion. Fox *et al*. [7] studied about the effects of yttrium on oxidation of Fe-5% Al alloy. They showed that convolution of oxide scale due to growth stress was not found when yttrium was present. Golightly *et al*. [8] compared the oxidation behavior of Fe-27% Cr-4% Al and Fe-27% Cr-4% Al-0.82% Y in 1 atm oxygen at 1200 °C. According to their results, the addition of yttrium to the alloy apparently prevent the formation of oxide within an existing oxide layer, improving the adherence of alumina scale.

Many investigators have studied to find mechanisms for the improved oxide scale adherence and mechanical properties due to the presence of reactive elements such as Y, Ce, and Hf, etc. The mechanisms reported previously can generally be categorized into seven groups: (1) pegging mechanism [9–11], (2) vacancy sink mechanism [12–14], (3) graded seal [15], (4) improvement of bond strength at the interface [16–18], (5) modification of growth process [16, 19–20], (7) and enhancement of scale plasticity [4, 6]. However, there exists no consensus view on the role of reactive elements in high-temperature oxidation of alloys.

The purpose of the present study is to investigate the effects of yttrium addition on the oxidation behavior of iron-aluminum alloys in terms of the oxidation rate, scale adhesion and microstructure.

2. Experimental procedure

2.1. Materials and sample preparation

The alloys used in this study were made by arc melting furnace, and subsequently homogenized at 1000 °C in

Ar atmosphere for 10 hrs. These were cut into elliptical shapes with a dimension of $\sim 1.7 \times 1.0 \times 0.1$ cm by a sectioning saw, and a hole was drilled to hang the specimen to microbalance using Pt wire. The samples were then abraded and polished through 1 μm diamond paste. After polishing, each specimen was degreased with soap and finally cleaned in an ultrasonic cleaner containing acetone. DCP (Double Current Plasma) and EPMA (Electron Microprobe Analysis) analyses were performed to examine the composition of the specimens. The composition of the two alloys used in this study are Fe-(14.33 wt%) Al and Fe-(14.08 wt%) Al-(0.30 wt%) Y.

2.2. Oxidation tests

The experimental set-up including TGA (Thermogravimetric Apparatus), shown schematically in Fig. 1, consisted of a recording electrobalance, a kanthal-wound furnace, and a gas train for purification and mixing of reagent gases. The argon and oxygen were dried and purified by passage through columns of P_2O_5 and ascarite. The alloy specimen was loaded with Pt wire into the reaction tube. Using a four-way stopcock, the argon gas was fed into the reaction tube while the argon/oxygen mixture flowed to the gas outlet at the same rate through the stopcock. After the temperature in the reaction tube reached 800, 900, and 1000 °C, the stopcock was reversed to feed the argon/oxygen gas-mixture into the reaction tube. From this point, the weight change of the sample was measured using an electrobalance (D101 Cahn balance) which has 1 μg sensitivity. Oxidation was carried out in 0.2 atm O_2 at 800, 900, and 1000 °C for 63 hrs. The parabolic oxidation rate constant was obtained by the least square method from the kinetic data. The adhesion of the oxide formed on the alloys was examined by thermal quenching and water impact in ultrasonic cleaner. Microstructure characterization and morphology examination were made by XRD (X-ray Diffraction), SEM (Scanning Electron Microscopy), EPMA (Electron Microprobe Analysis), and optical metallography.

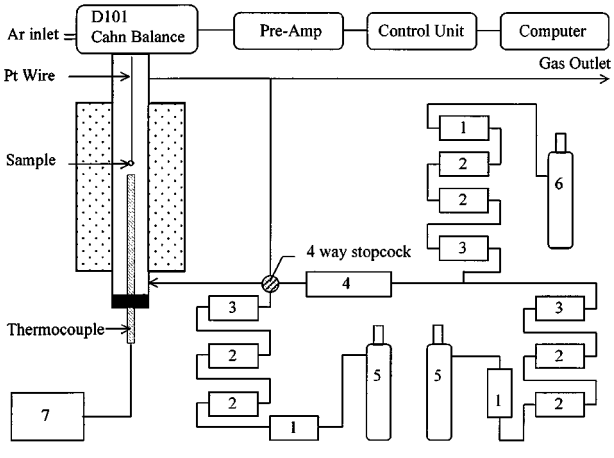

Figure 1 Schematic diagram of thermogravimetric apparatus (1. Ascarite (CO_2 removal), 2. P_2O_5 (H_2O removal), 3. Flowmeter, 4. Mixing chamber, 5. Ar cylinder, 6. O_2 Cylinder and 7. Thermometer).

3. Results & discussion

3.1. Oxidation rate

Oxidation experiments of the two alloys, Fe_3Al and Fe_3Al-Y, were carried out in 0.2 atm O_2 at 800, 900, and 1000°C. The change of specimen weight with time during the oxidation of Fe_3Al at 800, 900, and 1000 °C is shown in Fig. 2. It was observed that under the same experimental conditions the oxidation rate of Fe_3Al-Y alloy was almost same as that of Fe_3Al.

The oxidation rates of the two alloys were calculated using parabolic rate equation given by Equation 1

$$X^2 = K_p t \tag{1}$$

where X is the change in weight per unit surface area after time t, and K_p is parabolic rate constant. The parabolic rate constant obtained at 800 °C is 5.7×10^{-5} mg^2/cm^4 hr, which is consistent with the results of Devan [21], although the oxidizing atmosphere was slightly different. Table I shows the parabolic rate constants obtained at three different temperatures. As expected, oxidation rate is increased with increasing temperature. The temperature dependence of the parabolic rate constant (K_p) at constant oxygen pressure can be expressed by Equation 2.

$$K_p = K_o \exp\left(\frac{-Q}{RT}\right) \tag{2}$$

where K_o is a constant, Q activation energy, R gas constant, and T absolute temperature. The activation energy Q and the constant K_o were determined from a plot of log K_p vs. $1/T$ as shown in Fig. 3. The general

TABLE I Parabolic rate constants measured for Fe-14.3 wt% Al alloy at three temperatures

Temperature (K)	Parabolic Rate Constants (mg^2/cm^4 hr)
1073	5.7×10^{-5}
1173	1.3×10^{-4}
1273	1.1×10^{-3}

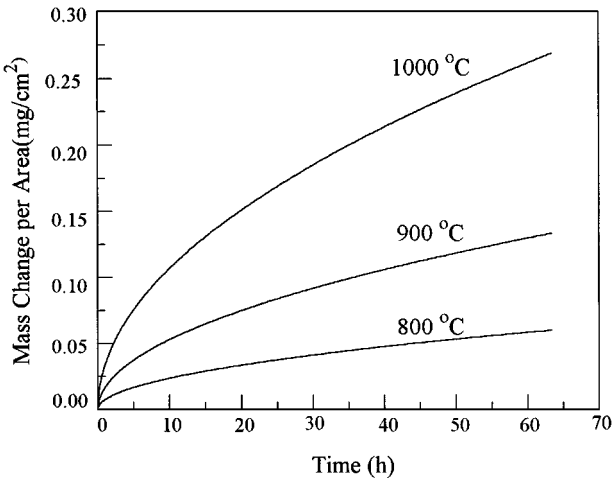

Figure 2 Weight-gain kinetictics for the oxidation of Fe-(14.3 wt%) Al alloy in 0.2 atm O_2 at 800, 900, and 1000 °C.

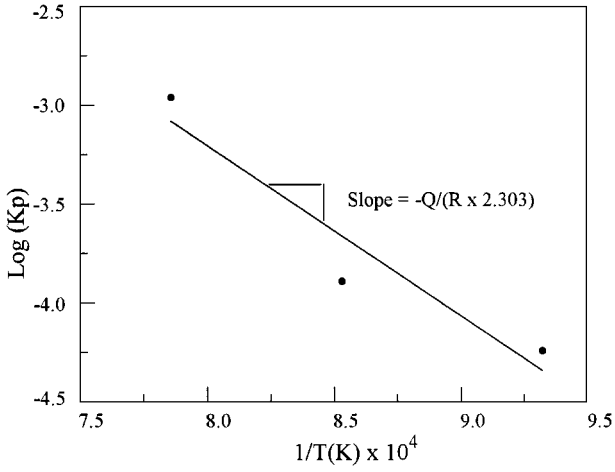

Figure 3 Temperature dependence of parabolic rate constants for the oxidation of Fe-(14.3 wt%) Al in 0.2 atm O_2 at 800, 900, and 1000 °C.

equation for the parabolic rate constant as a function of temperature is as follows:

$$K_p = 5128 \exp\left[\frac{-39506(\text{cal/mol})}{RT}\right] \text{mg}^2/\text{cm}^4\,\text{hr}$$

3.2. Oxide adhesion & microstructure

The oxides formed on Fe_3Al and Fe_3Al-Y were found to be K-Al_2O_3 at 800 °C and α-Al_2O_3 at 900, 1000, and 1100 °C. Fig. 4 shows the XRD patterns for the yttrium-free Fe_3Al alloys oxidized in 0.2 atm O_2 at 800, 900 and 1000 °C. In order to examine the adhesion of alumina scale to the substrate, the two alloy specimens oxidized at 800 and 900 °C were quenched in air at room temperature. The optical examination of the two specimens did not show any spallation of the oxide scale. The two alloys oxidized at the two temperatures were placed in an ultrasonic cleaner to further examine the degree of scale adhesion. The scale surface of the two oxidized specimens was impacted by water molecules via ultrasonic waves for 5 minutes. It was observed that while the alumina scale formed on Y-free Fe_3Al was cracked and spalled, Y-doped Fe_3Al maintained adhesive alumina scale without showing any cracks and spallation. Fig. 5A and B show the surface morphology of the two alloys oxidized at 1100 °C for 24 hrs. Oxide layer formed on the Y-free Fe_3Al (Fig. 5A) was severely convoluted and the alloy substrate was partially exposed due to the spallation of the oxide layer, indicating that the oxide scale was subjected to growth stress during oxidation and thermal stress during cooling. Meanwhile, oxide layer formed on the Fe_3Al-Y alloy was observed to be flat, dense, and adhesive. It is interesting to note that a second phase was observed on the surface of alumina scale formed on the Fe_3Al-Y as shown in Fig. 5B. The second phase will be discussed later in detail.

Fig. 6A and B show the oxide/substrate interface near the substrate and the substrate surface of the Y-free Fe_3Al oxidized at 1100 °C, respectively. As shown in the figures, the interface is wavy and the surface of the

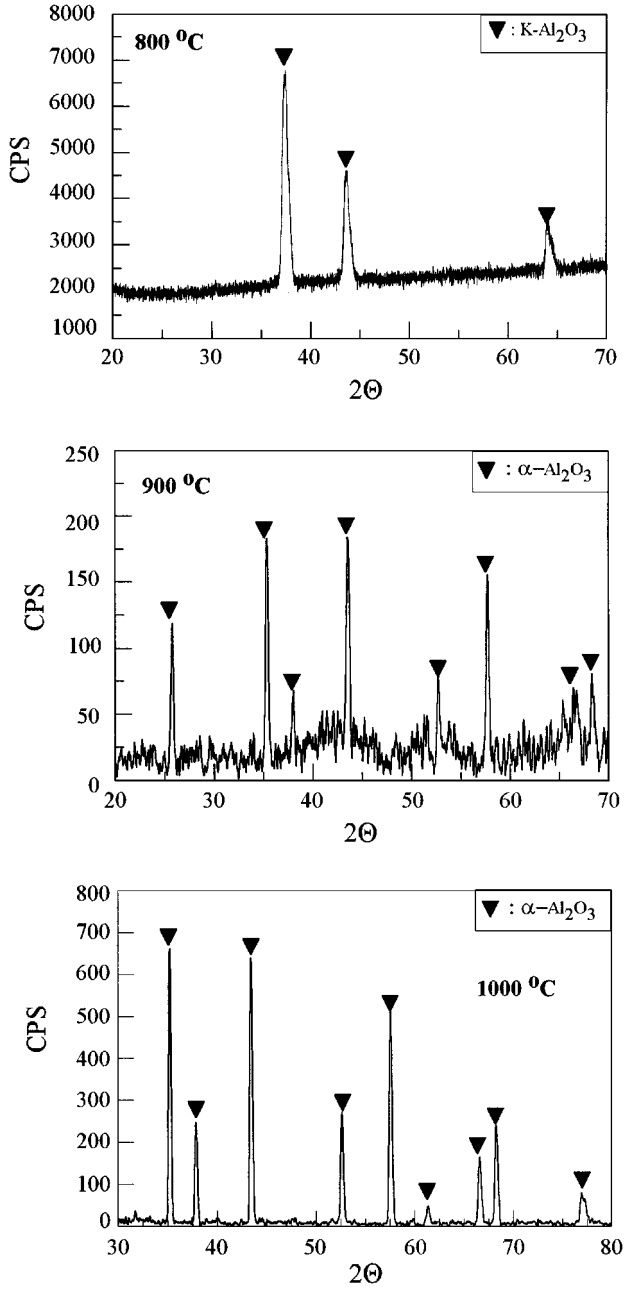

Figure 4 XRD results showing the phases of Al_2O_3 formed on Fe-(14.3 wt%) Al at 800, 900 and 1000°C.

substrate is deformed due to the stresses generated during the oxidation and cooing. On the other hand, the oxide/substrate interface of Fe_3Al-Y alloy oxidized at the same temperature seems to be straight without deformation, as shown in Fig. 7. From these observations, it may be deduced that the addition of yttrium to the alloy generates less stresses which may partly contribute to the enhancement of scale adhesion.

The surface of alumina scale formed on the Y-doped Fe_3Al was examined at various oxidation periods using optical microscope. As shown in Fig. 8A, yttrium is observed mainly at the grain boundaries of Fe_3Al-Y alloy before oxidation. As soon as the specimen is exposed to air at high temperature, the yttrium is oxidized to form a complex Y-Al oxide. As the oxidation proceeds, the appearance of the surface of the oxidized specimen remains same, as shown in Fig. 8C and D. The second phase, which is a complex Y-Al oxide, formed at the

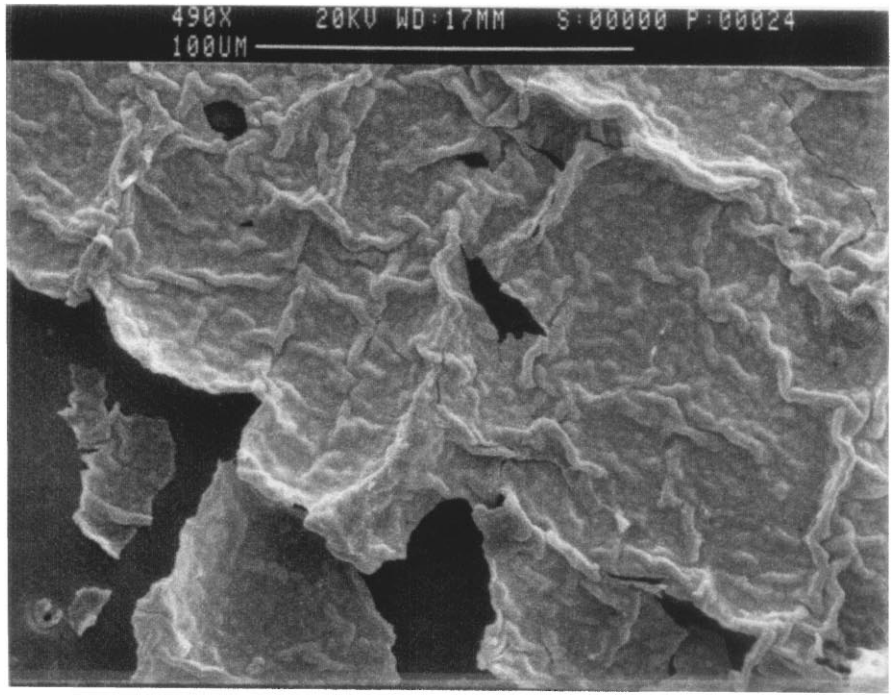

(A)

(B)

Figure 5 SEM micrographs showing the surface of (A) Fe-14.3 wt% Al and (B) Fe-14.1 wt% Al-0.3 wt% Y alloys oxidized in air at 1100 °C.

surface of alumina scale is shown in Fig. 9 and previously in Fig. 5, and is founded to be enriched with yttrium and oxygen by X-ray map and EPMA analyses. According to the XRD pattern shown in Fig. 10, the second phase seems to be $Y_3Al_5O_{12}$. The scale appearances shown in Fig. 8 indicate that the alumina scale formed on Fe_3Al-Y does not seem to grow externally but internally by inward oxygen diffusion through alumina scale.

The other phenomenon observed from the oxidation of Fe_3Al-Y alloy is the formation of pegs at the scale/substrate interface. Fig. 11 shows a typical peg formed at the alloy/scale interface. The pegs seem to be connected to the grain boundaries of the alloy substrate, implying that the pegs may be grown inward through the grain boundaries of the substrate. Also, the pegs anchor the oxide scale to the alloy substrate, leading to the improved scale adhesion. The analysis of X-ray map shown in Fig. 12 reveals that the pegs are enriched with O, Al, and Y, and deficient in iron. From this result, it can be concluded that the pegs are developed at the grain boundaries of the substrate near

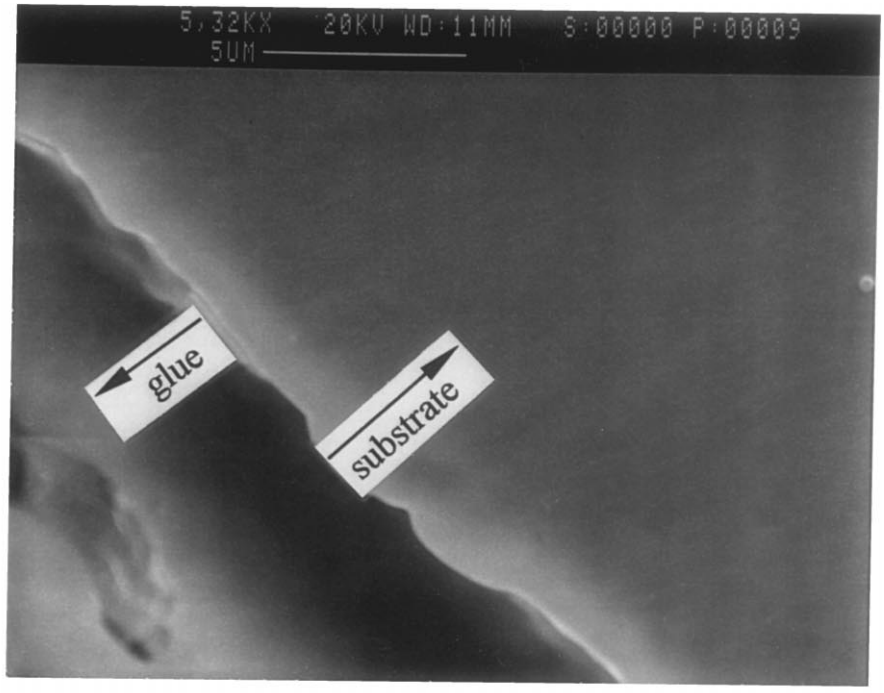

(A)

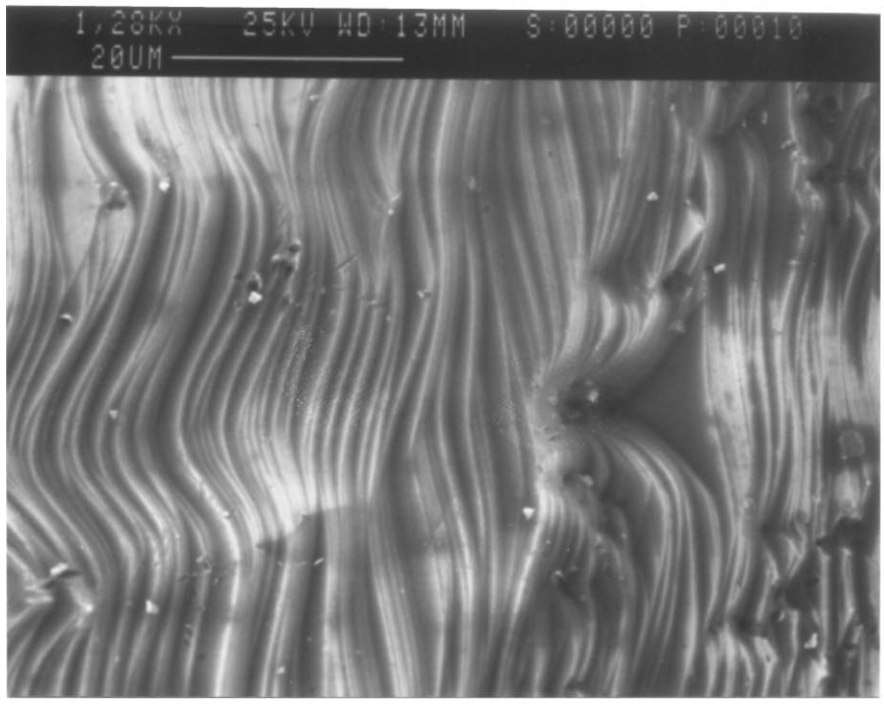

(B)

Figure 6 SEM micrographs showing (A) cross-section and (B) surface of Y-free Fe_3Al alloy substrate oxidized at 1100 °C in air for 120 hrs (oxide is removed).

the scale/substrate interface due to internal oxidation. In other words, oxygen diffuses inward through the alumina scale and reacts with Al and Y at the grain boundaries of the substrate to form new complex oxides like pegs in the substrate. Therefore, it can be deduced that the formation of pegs due to the presence of yttrium is indicative of the change of oxide growth mechanism.

Many studies have been carried out on the growth mechanism of alumina scale. Pint *et al*. [22] conducted sequential oxidation experiments of undoped, and Y- and Zr-doped β-NiA1 and FeCrAl alloys using ^{16}O and ^{18}O at 1200 and 1500 °C. According to these authors, undoped α-$A1_2O_3$ was found to grow by the simultaneous transport of both Al and O. On the other hand, Y- and Zr-doped α-$A1_2O_3$ was found to grow mainly by the inward transport of oxygen. Schumann *et al*. [23] investigated the oxide growth processes and interfacial segregation occurring in α-$A1_2O_3$ scales grown on β-NiAl containing Zr or Y at 1200 °C. They showed

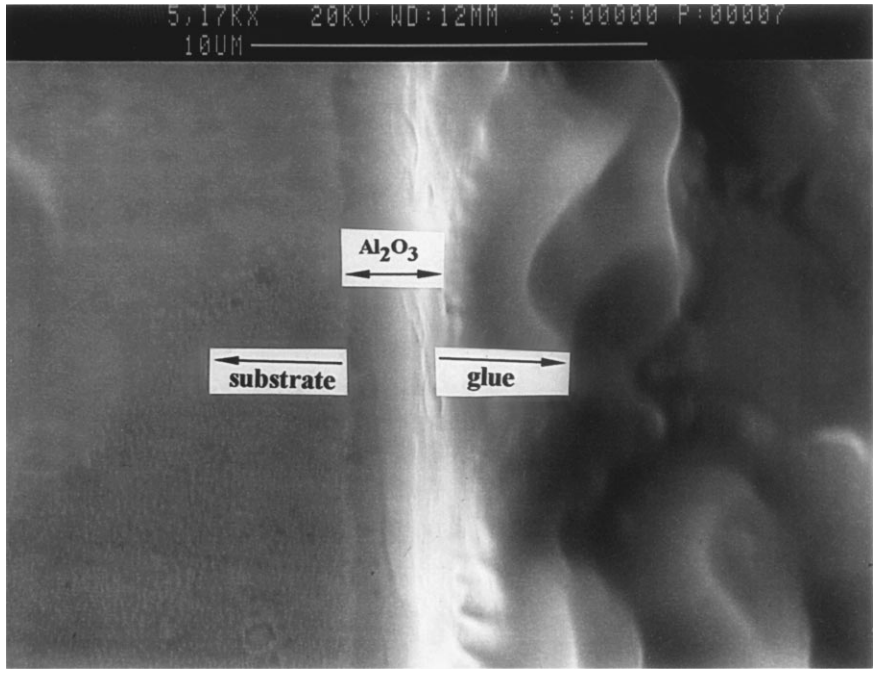

Figure 7 SEM micrograph showing the cross-section of Fe_3Al-Y alloy oxidized at 1100 °C in air for 120 hrs.

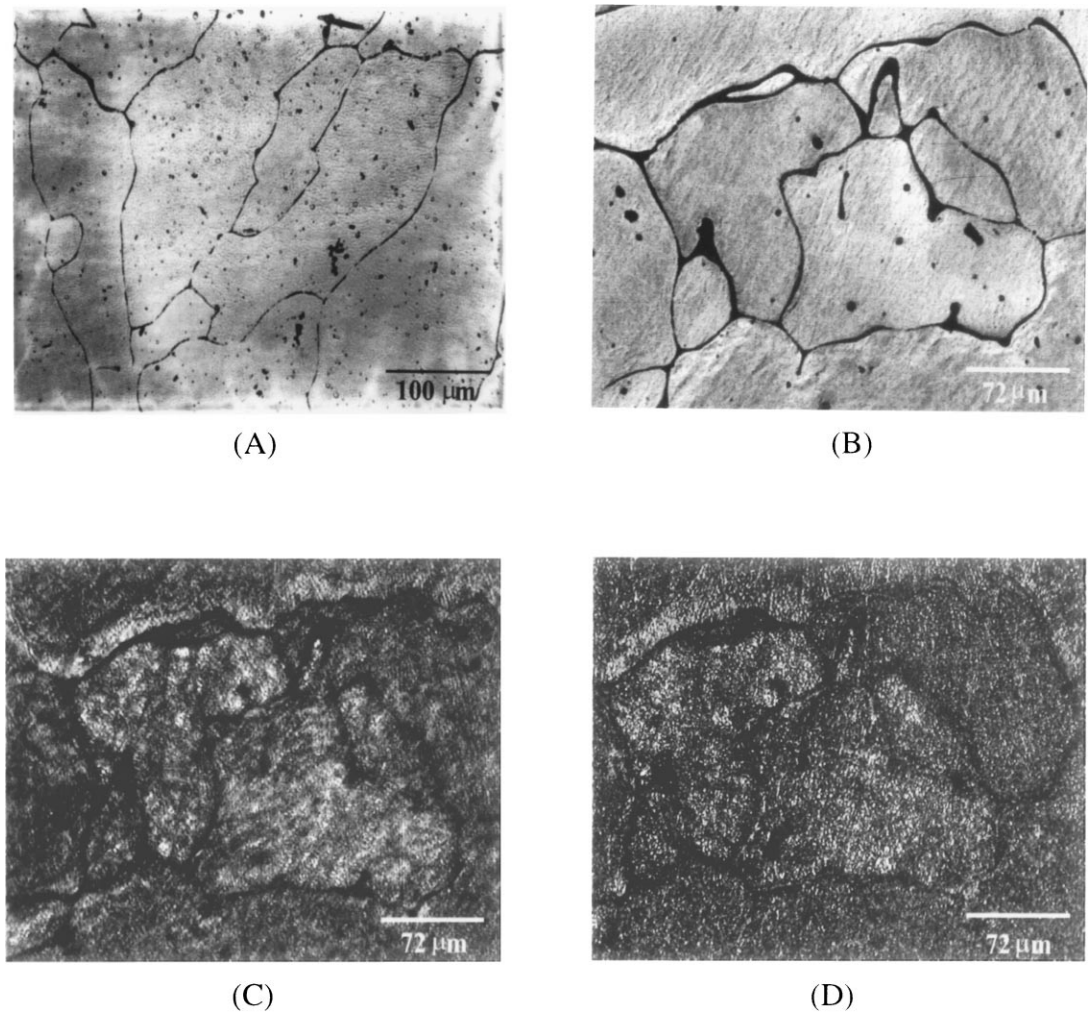

Figure 8 Change of surface appearance showing grain boundaries containing complex Y-Al oxide with time during oxidation of Fe_3Al-Y in air at 1100 °C: (A) surface of Fe_3Al-Y etched in 90 ml H_2PO_3-8 ml HNO_3-2 ml H_2O solution before oxidation (B) after oxidation for 4 min (C) after oxidation for 80 hrs (D) after oxidation for 320 hrs.

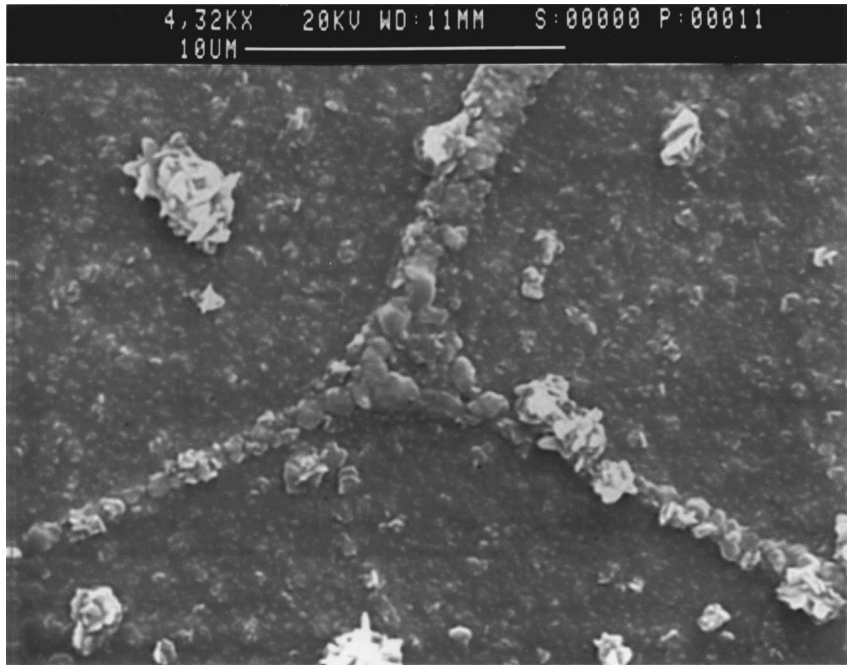

Figure 9 SEM micrograph showing a yttrium oxide protruded on the surface of α-Al_2O_3 formed for the oxidation of Fe_3Al-Y alloy in air at 1100 °C.

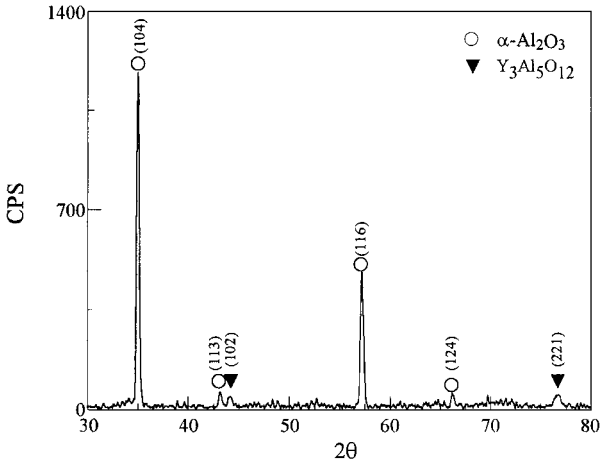

Figure 10 XRD results showing the phases of oxide formed on Fe_3Al-Y at 1100 °C.

that the extent of aluminum diffusion occurring during α-$A1_2O_3$ growth was reduced by the presence of alloying elements and thus the oxide grew by inward diffusion of oxygen. Prescott *et al*. [24] investigated the growth mechanism of alumina scale formed on Fe-25 wt% Al and reported that α-Al_2O_3 grew by simultaneous countercurrent diffusion of Al and oxygen.

The formation of alumina by the simultaneous countercurrent diffusion of aluminum and oxygen indicates that growth stress can be generated in the scale during the growth of alumina scale, which may lead to spallation of alumina scale. On the other hand, the addition of yttrium to the Fe_3Al changes the oxide growth mechanism from the simultaneous countercurrent diffusion of aluminum and oxygen to predominant oxygen diffusion, which leads to the formation of scale and pegs at the alloy/scale interface. Accordingly, the

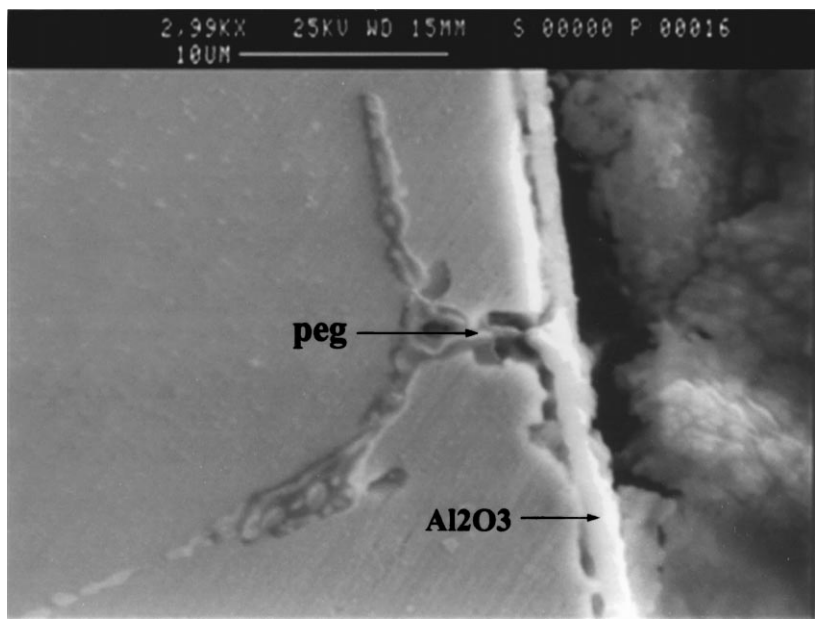

Figure 11 SEM micrograph showing the formation of peg at Al_2O_3/Fe_3Al-Y interface.

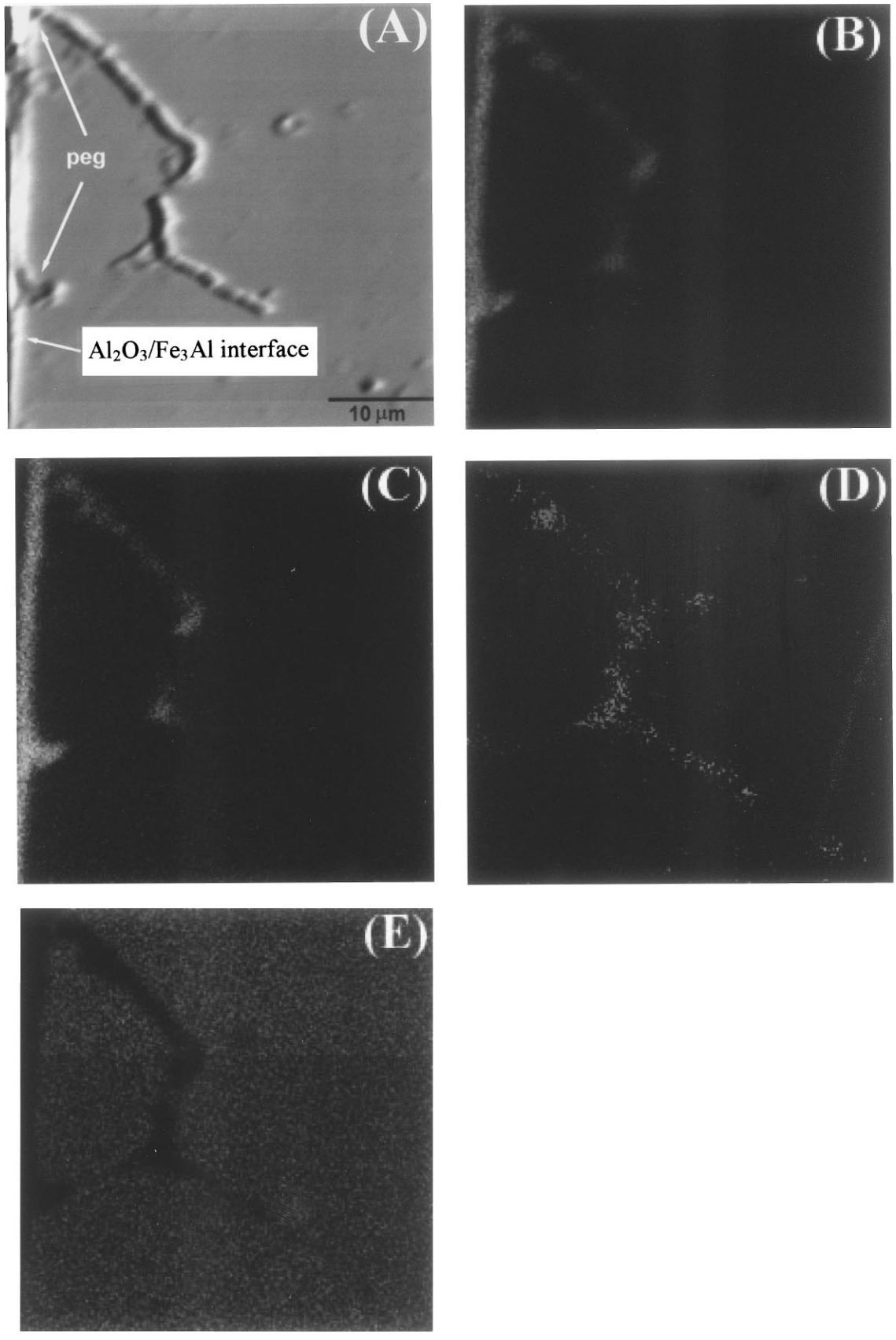

Figure 12 SEM and X-ray maps showing the composition of pegs formed at alumina scale/substrate interface: (A) SEM image, (B) oxygen x-ray map, (C) aluminum x-ray map, (D) yttrium x-ray map, and (E) iron x-ray map.

Fe_3Al-Y alloy is subjected to less growth stress during the oxidation and is more resistant to thermal stress during cooling, which results in enhanced oxide adhesion and stability.

4. Conclusions

1. The oxidation rates of Fe_3Al and Fe_3Al-Y alloys in the temperature range of 800°C to 1000 °C were nearly identical and the general equation for the parabolic rate

constants as a function of temperature can be expressed as $K_p = 5128 \exp[-39506\ (\text{cal/mol})/RT]\ \text{mg}^2/\text{cm}^4\ \text{hr}$.

2. The addition of small amount of yttrium to Fe_3Al alloy modifies the oxide growth mechanism from countercurrent diffusion of aluminum and oxygen to predominant oxygen diffusion. The change of growth mechanism leads to the formation of pegs and less oxide growth stress which enhances the adhesion of alumina scale to the alloy substrate.

References

1. G. WALLWORK and A. HED, *Oxid. Met.* **3** (1971) 171.
2. G. SAUTHOFF, "Intermetallics" (Weinheim, New York, 1995) p. 13.
3. C. S. TEDMON, *J. Electrochem. Soc.* **113** (1966) 766.
4. T. A. RAMANARAYANAN, M. RAGHAVAN and R. PETKOVIC-LUTON, *ibid.* **131** (1984) 923.
5. *Idem., Oxid. Met.* **22** (1984) 83.
6. T. A. RAMANARAYANAN, R. AYER, R. PETKOVIC-LUTON and D. P. LETA, *ibid.* **29** (1988) 445.
7. P. FOX and G. J. TATLOCK, *Mater. Sci. Technol.* **4** (1988) 439.
8. F. A. GOLIGHTLY, F. H. STOTT and G. C. WOOD, *Oxid. Met.* **10** (1976) 163.
9. K. L. LUTHRA and C. L. BRIANT, *ibid.* **26** (1986) 397.
10. J. NOWOK, *ibid.* **18** (1982) 1.
11. Y. SAITO and T. MARUYMA, *Mat. Sci. Eng.* **87** (1987) 275.
12. M. W. BRUMM and H. J. GRABKE, *Corros. Sci.* **34** (1993) 547.
13. S. C. CHOI, H. J. CHO and D. B. LEE, *Oxid. Met.* **46** (1996) 109.
14. C. S. GIGGINS and F. S. PETTIT, *Metall. Trans.* **2** (1971) 1071.
15. J. PETERS and H. J. GRABKE, *Werkst. Korros.* **35** (1984) 385.
16. A. B. ANDERSON and S. P. MEHANDRU, *J. Electrochem. Soc.* **132** (1985) 1695.
17. L. L. KRISHAN and CLYDE L. BRIANT, *Oxid. Met.* **26** (1986) 397.
18. J. E. MCDONALD and J. G. EBERHART, *Trans. AIME* **233** (1965) 512.
19. G. B. ABDERRAZIK, G. MOULIN and A. M. HUNTZ, *Solid State Ionics* **22** (1987) 285.
20. *Idem., Oxid. Met.* **33** (1990) 237.
21. J. H. DEVAN, in "Oxidation of High-Temperature Intermetallics," edited by T. Grobstein and J. Doychak (TMS, Warrendale, PA, 1989) p. 107.
22. B. A. PINT, J. R. MARTIN and L. W. HOBBS, *Oxid. Met.* **39** (1993) 167.
23. E. SCHUMANN, J. C. YANG, M. RUHLE and M. J. GRAHAM, *ibid.* **46** (1996) 37.
24. R. PRESCOTT, D. F. MITCHELL, G. I. SPROULE, R. J. HUSSEY and M. J. GRAHAM, in "High Temp. Corros. Adv. Mater. Prot. Coat.," edited by S. Yasutoshi (North-Holland, Amsterdam, Neth.,1992) p. 83.

Received 14 April 1999
and accepted 3 February 2000